Published in final edited form as:
J Immunol. 2018 February 01; 200(3): 1159–1168. doi:10.4049/jimmunol.1700965.

ATP evokes Ca^{2+} responses and CXCL5 secretion via $P2X_4$ receptor activation in human monocyte-derived macrophages

Janice A. Layhadi[*], **Jeremy Turner**[†], **David Crossman**[‡], and **Samuel J. Fountain**[*]

[*]School of Biological Sciences, University of East Anglia, Norwich Research Park, UK

[†]Elsie Bertram Diabetes Center, Norfolk and Norwich University Hospital, Norwich, UK

[‡]School of Medicine, University of St Andrew's, UK

Abstract

Leukocytes sense extracellular ATP, a danger-associated molecular pattern, released during cellular stress and death, via activation of cell surface P2X and P2Y receptors. Here, we investigate P2 receptor expression in primary human monocyte-derived macrophages and receptors that mediate ATP-evoked intracellular $[Ca^{2+}]_i$ signals and cytokine production in response to ATP concentrations that exclude $P2X_7$ receptor activation. Expression of $P2X_1$, $P2X_4$, $P2X_5$, $P2X_7$, $P2Y_1$, $P2Y_2$, $P2Y_4$, $P2Y_6$, $P2Y_{11}$ and $P2Y_{13}$ was confirmed by qRT-PCR and immunocytochemistry. ATP elicited intracellular Ca^{2+} responses in a concentration-dependent fashion (EC_{50} = 11.4 ± 2.9 μM, N=3). $P2Y_{11}$ and $P2Y_{13}$ activations mediated the amplitude of $[Ca^{2+}]_i$ response, whilst $P2X_4$ activation, but not $P2X_1$ or $P2X_7$, determined the duration of Ca^{2+} response during a sustained phase. ATP-mediated gene induction of CXCL5, a pro-inflammatory chemokine. $P2X_4$ antagonism (PSB-12062 or BX-430) inhibited ATP-mediated induction of CXCL5 gene expression and secretion of CXCL5 by primary macrophage. Inhibition of CXCL5 secretion by $P2X_4$ antagonists was lost in the absence of extracellular Ca^{2+}. Reciprocally, positive allosteric modulation of $P2X_4$ (ivermectin) augmented ATP-mediated CXCL5 secretion. $P2X_7$, $P2Y_{11}$ or $P2Y_{13}$ receptor did not contribute to CXCL5 secretion. Together, the data reveals a role for P2X4 in determining the duration of ATP-evoked Ca^{2+} responses and CXCL5 secretion in human primary macrophage.

Keywords

$P2X_4$; ATP; CXCL5; purinergic receptors; human macrophages; pro-inflammatory chemokines

Introduction

ATP is a danger-associated molecular pattern (DAMP) released during cellular stress and cell death at sites of inflammation and injury (1–3). The extracellular ATP DAMP signal can be sensed by leukocytes and mediates physiological responses via activation of cell surface P2 receptors: ligand-gated cation channel P2X ($P2X_{1-7}$) receptors and G-protein coupled

To whom correspondence should be addressed: Dr Samuel Fountain, School of Biological Sciences, University of East Anglia, Norwich Research Park, NR4 7TJ, UK, Telephone: +44(0) 1603597326; s.j.fountain@uea.ac.uk.

Europe PMC Funders Author Manuscripts

P2Y ($P2Y_{1,2,4,6,11-14}$) receptors (4). While the main agonist for P2X receptors is ATP, there are five major native ligands for P2Y receptors: ATP ($P2Y_2$, $P2Y_{11}$), ADP ($P2Y_1$, $P2Y_{12}$ and $P2Y_{13}$), UTP ($P2Y_2$, $P2Y_4$), UDP ($P2Y_6$) and UDP-glucose ($P2Y_{14}$) (5). The activation of ligand-gated P2X receptors leads to a direct increase in intracellular Ca^{2+} level. P2Y receptors, however, involve a more complex downstream signaling pathway with activation of G_q-coupled receptors ($P2Y_{1,2,4,6,11}$) resulting in activation of PLC/IP_3 pathway leading to increased Ca^{2+} concentration through release of stored ER Ca^{2+} and capacitative influx pathways, and activation of G_i-coupled ($P2Y_{12-14}$) P2Y receptors resulting in inhibition of adenylate cyclase (AC) and reduction in cyclic AMP (cAMP) level (6).

$P2X_1$, $P2X_4$ and $P2X_7$ are commonly coexpressed by leukocytes (7, 8). $P2X_1$ and $P2X_4$ are maximally activated by low micromolar ATP levels (9), whilst the activation threshold for $P2X_7$ is at much higher ATP concentration (>500 μM) (10–13). Although the role of $P2X_7$ receptor activation in leukocytes has received significant attention (14–19), the cellular role of $P2X_4$ is less well understood. Some evidence in mouse macrophage has emerged for the involvement of $P2X_4$ in the release of inflammatory mediators like prostaglandin E_2 (PGE_2) (20) and in $P2X_7$-mediated autophagy (15). More recently, it was reported that $P2X_7$-mediated inflammation in mouse macrophage cell line is regulated by co-expression with $P2X_4$ through facilitation of IL-1β release (14). Interaction between $P2X_4$ and $P2X_7$ receptors have also been described as an important determinant of macrophage phenotypic function and their role in clearance of apoptotic cells following tissue damage (21). Despite these efforts, a functional role of the $P2X_4$ receptor in human macrophage remained elusive.

In the context of inflammation, macrophages possess three key roles which include antigen presentation, phagocytosis and immunomodulation through the production of cytokines, chemokines and growth factors (22). Cytokines and chemokines are potent signaling molecules that are produced by many cell types primarily those of the immune system and have key roles in mediating cell-to-cell communication (23). Other roles of these proteins include the regulation of local and systemic inflammation to chemotaxis, tissue repair, cellular proliferation and metabolism (23). In humans, CXC ligand (CXCL) 5/ENA-78 is a pro-inflammatory chemokine that regulates CXCR2-dependent neutrophil trafficking. It is believed that platelets serve as the main source of CXCL5 under homeostatic conditions, however, during severe infection, CXCL5 is produced predominantly by lung epithelial cells (24, 25). In addition to this, a study has illustrated high levels of expression and secretion of the chemokine CXCL5 in the tissue-resident macrophage population of white adipose tissue (26). Despite being secreted by various cells, it has not been reported if human macrophages are able to secrete CXCL5 upon sensing DAMP signals such as ATP, and to what end purinergic receptors play in this mechanism.

Here, we studied the functional role of $P2X_4$ receptor in human primary monocyte-derived macrophages (MDMs) as a surrogate cell model of primary tissue macrophages. Though studies have revealed some differentially expressed genes (27, 28) and proteins (29, 30), MDMs differentiated through treatment with GM-CSF have been typically considered to be phenotypically and ‘behaviourally’ similar to human lung macrophages (31–33). In the lung, MDMs are recruited following inflammation in a C-C chemokine receptor type 2 (CCR2)-dependent manner (34) and have been shown to exacerbate pulmonary fibrosis in mice (35–

41). In addition to this, it has also been shown that increased CXC chemokine levels may serve as important pathogenetic mediators of pulmonary fibrosis (42, 43).

In the present study, several key questions were investigated: 1) the identification of purinergic receptors (P2X and P2Y) expressed in human MDMs, 2) characterization of purinergic receptors contributing to ATP-evoked intracellular Ca^{2+} ($[Ca^{2+}]_i$) response in macrophages and finally, 3) elucidating a functional role of $P2X_4$ receptor in human macrophages, particularly its roles in cytokine/chemokine production.

Materials and Methods

Chemicals and reagents

The following reagents were used: PSB-12062 and ATP (Sigma-Aldrich, USA), A438079 (Abcam, UK), 5-BDBD, MRS-2578, BX430, Ivermectin, Ro0437626, NF340, MRS-2211, Arc-118925xx, MRS2500, U-73122 (all from Tocris, USA), recombinant human GM-CSF (rhuGM-CSF) (Peprotech, USA) and Fura-2AM (TefLabs, USA).

Generation of $hP2X_4$ and $hP2X_7$ over expressing 1321N1 cells

Generation of over-expressing cells were performed in house. Blank 1321N1 astrocytoma cells (2.5×10^5) were transduced with $hP2X_4$ mCherry or $hP2X_7$ mCherry lentiviral particles using spinoculation method (1,600 *x g*; 60 minutes; 22°C). Supernatant was slowly aspirated and cells were gently resuspended in cell culture media to allow recovery in a T75 flask. Success of transduction was confirmed by visualization under fluorescence microscopy. To obtain highly expressing cells, transduced 1321N1 were sorted using BD FACSAria. All concentration responses and inhibition curves were performed in cells with low passages (P1-P4 cells) to ensure maximal response.

Isolation of PBMCs and generation of monocyte-derived macrophages

Peripheral venous blood was collected from healthy human volunteers through the National Health Service (NHS) Blood and Transplant (Addenbrooke's Hospital, Cambridge University Hospital, Cambridge, UK). Blood was layered on top of Histopaque-1077 (Sigma-Aldrich, UK) for centrifugation at 1000 x g for 25 min. Buffy coat layers was collected and PBMCs were counted. Cells were allowed to adhere onto T75 flasks (Corning, UK) for 2h and cultured in RPMI-1640 with 2mM L-glutamine, 2.5% heat-inactivated autologous serum and 50 IU/ml penicillin and 50 μg/ml streptomycin at 37°C, for 6d with 10 ng/ml rhuGM-CSF (Peprotech, USA).

Intracellular Ca^{2+} measurements

Cells were loaded for 1h with Fura-2 AM and treated with antagonists for 30 min. Measurements were made on a 96-well plate reader (FlexStation III, Molecular Devices). Change in $[Ca^{2+}]_i$ concentration is indicated as ratio of Fura-2 emission intensities at 340- and 380-nm (F ratio). SBS buffer contained (mM): 130 NaCl, 5 KCL, 1.2 $MgCl_2$, 1.5 $CaCl_2$, 8 D-glucose, 10 HEPES pH 7.4. Ca^{2+}-free SBS was prepared by excluding $CaCl_2$ and supplemented with 2 mM EGTA. Loading of cells with Fura-2 was performed in SBS buffer supplemented with 0.01% (w/v) pluronic acid.

ATP stimulation of monocyte-derived macrophages

MDMs were detached using TrypLE™ Express (Thermo Fisher). Cells (1 mL at $0.5x10^6$/mL) were stimulated with either vehicle, antagonists or modulators for 30 min followed by stimulation with 100 μM ATP for various time points (6, 9, 18, 24, 32 or 48h). Supernatants were collected at different time points and cells were lysed using TriReagent (Sigma-Aldrich) for RNA extraction.

Flow cytometry

Cells (100 μL at $1x10^6$/mL) were incubated for 10 min at room temperature (RT) with Fc block (BD, USA) and immunostained with anti-human CD14 PE or hIgG isotype control PE (both from BD, USA) before acquisition on the Cytoflex instrument (Beckman Coulter, USA). Positive staining was assessed based on gating of negative control (isotype control). Analyses were performed on CytExpert software.

Real-time RT-PCR analysis

Total RNA was isolated from cells using TRI Reagent (Sigma Aldrich) and contaminating genomic DNA was eliminated using DNA-free kit (Ambion). cDNA was synthesized from 0.5 μg of total RNA using SuperScript II reverse transcriptase kit (Invitrogen). Taqman primer probes sets for human CXCL5 (Hs01099660_g1), $P2X_1$ (Hs00175686_m1), $P2X_2$ (Hs04176268_g1), $P2X_3$ (Hs01125554_m1), $P2X_4$ (Hs00602442_m1), $P2X_5$ (Hs01112471_m1), $P2X_6$ (Hs01003997_m1), $P2X_7$ (Hs00175721_m1), $P2Y_1$ (Hs00704965_s1), $P2Y_2$ (Hs04176264_s1), $P2Y_4$ (Hs00267404_s1), $P2Y_6$ (Hs00366312_m1), $P2Y_{11}$ (Hs01038858_m1), $P2Y_{12}$ (Hs01881698_s1), $P2Y_{13}$ (Hs03043902_s1), $P2Y_{14}$ (Hs01848195_s1), GAPDH (Hs02758991_g1) and RPLP0 (Hs99999902_m1) were obtained predesigned from Applied Biosystems. Real-time RT-PCR was performed in a 7500 Fast Real-Time PCR instrument (Applied Biosystem). Target gene expression was normalized to GAPDH endogenous control and relative quantification was done by the ΔΔCT method.

RT^2 profiler PCR Array

Human Cytokines & Chemokines RT^2 Profiler PCR Array (Qiagen) was employed to screen 84 genes central to immune response according to manufacturer's instructions. Real-Time PCR was performed on 7500 fast instrument (Applied Biosystems). Values were corrected against the geometric mean of 5 housekeeping genes (ACTB, B2M, GAPDH, RPLP0 and HPRT1) and analysed using ΔΔCt method. Data was represented as heat map generated by Matrix2png and re-calculated as $\log_2$ fold change whereby the value 0 denotes no change in expression, positive value denotes upregulation and negative value denotes downregulation.

Luminex assay

The amount of proteins secreted in the supernatants of stimulated cells was quantified using either the Milliplex® MAP Kit Human Th17 Magnetic Bead Panel 96-well plate assay (IFN-γ, IL-17A, IL-6, IL-23, IL-17E, IL-27, IL-12(p70) and IL-33) or Milliplex® MAP Kit Human Cytokine/Chemokine Magnetic Bead Panel 96-well plate assay (IL-10, IL-8,

RANTES, Eotaxin, IL-13, IL-4, IL-5, IL-9 and MDC) (both from Millipore, UK) according to manufacturer's instructions.

ELISA

The amount of CXCL5 protein secreted in supernatants of stimulated cells was quantified using huCXCL5 ELISA kit (Biolegend, UK) according to manufacturer's instructions.

Immunocytochemistry

Cells (1 mL at $2.5x10^4$/mL) were fixed with 4% PFA (15 min, RT) and permeabilized with 0.25% Triton X-100 (10 min, RT). Cells were blocked with 1% BSA (30min, RT) and incubated overnight at 4°C with primary antibodies (rabbit polyclonal $P2X_{4,7}$ and $P2Y_{11,13}$ (Alomone, Israel), goat polyclonal $P2X_{1,5}$ and $P2Y_{12}$, and rabbit polyclonal $P2Y_{1,2}$ (Santa-Cruz Biotechnology, USA)). Cells were stained with secondary antibody goat anti-rabbit (Life Technologies, USA) or rabbit anti-goat (Abcam, UK) AF 488. Nuclear staining was performed with Vectashield Antifade containing DAPI (Vectorlabs, UK). Cell imaging were performed using laser-scanning confocal microscope Zeiss LSM510 META (Zeiss).

Data and Statistical Analysis

Data were analysed using Origin Pro 9.0 software (Origin Lab, USA). Concentration-response curves were fitted assuming a Hill coefficient of 1. Peak response was defined as the highest point of magnitude following agonist stimulation (represented by F ratio) while measurement of sustained phase was calculated using: 1) area under the curve (AUC) recorded between 0 and 230.4 seconds and 2) decay kinetics (τ) value. Hypothesis testing for experiments with paired datasets were performed by means of paired Student's *t*-test. Data are expressed as mean ± SEM.

Results

Monocyte-derived macrophages express a wide range of purinergic receptors at mRNA and protein level

Human primary MDMs were obtained by the differentiation of monocytes following 6d stimulation with rhu-GM-CSF. Morphological characteristics of these MDMs were confirmed through bright field image system, where the majority of the population had a round and granular 'fried-egg' structural feature (Figure 1A), a main hallmark of GM-CSF-derived MDMs (44–47). Forward (FSC) and side scatter (SSC) plot from flow cytometry illustrated that the MDM population makes up approximately 69.8 ± 5.1% of the entire culture population (P2 gate; Figure 1B, left panel). Further characterization of these cells using FACS analysis illustrated that only 70.5 ± 4.6% of the MDM population are $CD14^+$ (Figure 1B; right panel). This is not surprising as CD14 is a known surface marker of monocytes that is downregulated by GM-CSF upon differentiation towards macrophages at both the mRNA and protein level (48, 49).

Expression of purinergic receptors (P2X and P2Y) in MDMs were investigated at the mRNA and protein level. qRT-PCR analysis identified mRNA expression of all P2X genes with the exception of $P2X_2$, $P2X_3$ and $P2X_6$, and all P2Y genes with the exception of $P2Y_{12}$ and

$P2Y_{14}$ (Figure 1C). Exclusion for genes was defined so that genes amplified above cycle threshold 35 were determined as 'absent'. Using immunocytochemistry, protein expression of purinergic receptors in MDMs was also studied. $P2X_1$, $P2X_4$, $P2X_5$, $P2X_7$, $P2Y_1$, $P2Y_2$, $P2Y_6$, $P2Y_{11}$ and $P2Y_{13}$ were all expressed in MDMs with at the protein level. Meanwhile, no positive staining was observed for $P2Y_{12}$ receptor in the MDM.

$P2Y_{11}$ and $P2Y_{13}$ receptor activation mediates the amplitude of ATP-evoked $[Ca^{2+}]_i$ response in human MDMs

ATP evoked a concentration-dependent increase in $[Ca^{2+}]_i$ response in both the presence and absence of extracellular Ca^{2+} (EC_{50} = 11.4 ± 2.9 μM in presence of extracellular Ca^{2+} *vs.* EC_{50} = 9.77 ± 2.4 μM in absence of extracellular Ca^{2+}) (Figure 2A). Responses to ATP (100 μM) were biphasic; an initial rapid $[Ca^{2+}]_i$ response which peaked and was followed by a modestly decaying sustained phase which returned to baseline level (Figure 2B). Throughout the study, 100 μM ATP was used as the agonist concentration, as our intracellular Ca^{2+} measurement data in over-expressing cells illustrated maximal activation of $P2X_4$ and no activation of $P2X_7$ (Supplementary Figure 1A and E).

Pre-incubation of MDMs with 10 μM phospholipase C inhibitor (U-73122) almost completely abolished the rapid peak in ATP-evoked $[Ca^{2+}]_i$ response (90.0 ± 0.96% inhibition, N=3, P<0.005) (Supplementary Figure 2E), indicating that the majority of the ATP-evoked $[Ca^{2+}]_i$ response in MDMs are dependent on PLC activation. To identify and characterize which receptors are crucial for ATP-evoked $[Ca^{2+}]$i response in MDMs, various P2Y receptor antagonists were tested. Pre-treatment of MDMs with $P2Y_1$ (MRS2500; 1 μM), $P2Y_2$ (ARC-118925xx; 10 μM), or $P2Y_6$ (MRS2578; 10 μM) antagonists had no significant effect on the amplitude of ATP-evoked $[Ca^{2+}]_i$ response (Supplementary Figure 2F-K). The amplitude of the ATP-evoked $[Ca^{2+}]_i$ response in MDMs was mediated by co-activation $P2Y_{11}$ and $P2Y_{13}$, as pre-treatment of MDMs with selective $P2Y_{11}$ antagonist (NF340; 10 μM) caused a 21.4 ± 5.1% inhibition (N=3, P<0.05, Figure 2C and F) and $P2Y_{13}$ antagonist (MRS2211; 10 μM) caused a significant inhibition of 30.4 ± 2.1% (N=3, P<0.001, Figure 2D and F). In the presence of both antagonists, ATP-evoked $[Ca^{2+}]_i$ response was significantly inhibited by 45.9 ± 4.3 % (N=3; P<0.001, Figure 2E and F).

$P2X_4$, but not $P2X_1$ or $P2X_7$, receptor activation contributes to the sustained phase of the ATP-evoked $[Ca^{2+}]_i$ response

To investigate if P2X receptors could also contribute to the ATP-evoked $[Ca^{2+}]_i$ response in MDMs, several P2X antagonists and modulators were tested. Pre-treatment of MDMs with a selective $P2X_1$ receptor antagonist (Ro0437626; 30 μM) did not have any inhibitory effect, in fact, it potentiated the amplitude of the ATP-evoked $[Ca^{2+}]_i$ response by 31.3 ± 11.4% (N=4, P<0.01) (Supplementary Figure 2A and B). Selective antagonism of $P2X_7$ receptor with (A438079; 5 μM) had no significant effect on the $[Ca^{2+}]_i$ response (Supplementary Figure 2C and D). Finally, the contribution of $P2X_4$ receptor towards ATP-evoked $[Ca^{2+}]_i$ response was tested using several pharmacological tools: a positive allosteric modulator, IVM (50), and selective antagonist, PSB-12062 (51) and BX-430 (52). Pre-treatment of MDMs with IVM (3 μM) significantly potentiated the amplitude of $[Ca^{2+}]_i$ response (18.2 ± 4.58% potentiation, N=12, P<0.01; Figure 3A) and significantly increased the net calcium

movement as quantified by area under the curve (198.81 ± 27.91% increase, N=12, P<0.01; Figure 3B). Pre-treatment of MDMs with PSB-12062 (10 μM) caused a very minor effect on the amplitude of the $[Ca^{2+}]_i$ response (7.7 ± 2.7% inhibition, N=12, P<0.05, Figure 3C) but had a more significant effect in inhibiting the duration of $[Ca^{2+}]_i$ response in response to ATP (38.97 ± 7.49 % inhibition, N=12, P<0.01, Figure 3D). Pre-treatment of MDMs with newly identified selective antagonist BX430 produced a similar effect to PSB-12062, whereby 5 μM BX430 had a minor effect on the peak magnitude of ATP-evoked Ca^{2+} response (Figure 3E), whilst significantly inhibiting net calcium movement (57.72 ± 12.65 % inhibition, N=5, P<0.05; Figure 3F). The co-application of $P2X_4$ antagonists (10 μM PSB-12062 or 5 μM BX430) was performed in the presence of both $P2Y_{11}$ antagonist (10 μM NF-340) and $P2Y_{13}$ antagonist (10 μM MRS-2211) to further illustrate the contribution of these receptors to ATP-evoked Ca^{2+} response in human MDMs. In the presence of $P2Y_{11}$ and $P2Y_{13}$ receptor antagonists, 5 μM BX430, but not 10 μM PSB-12062, resulted in a further inhibition of peak magnitude of the ATP-evoked Ca^{2+} response (45.88 ± 4.29 % inhibition without BX430 *vs.* 51.73 ± 2.85 % with BX430, N=4, P<0.0.5; Figure 3G and Supplementary Table 1). To provide further evidence that activation of $P2X_4$ receptor, but not $P2Y_{11}$ or $P2Y_{13}$ receptor, contributed towards the duration and shape of the Ca^{2+} response, decay kinetics of Ca^{2+} response in the presence of these antagonists were quantified. $P2X_4$ receptor antagonists (PSB-12062 or BX430) significantly increased response decay kinetics (Supplementary Table 1). Therefore, whilst $P2Y_{11}$ and $P2Y_{13}$ receptors activation contributes to the amplitude of the ATP-evoked $[Ca^{2+}]_i$ response in MDMs, the activity of $P2X_4$ receptor contributes to the duration of response.

ATP-mediated induction of cytokine and chemokine gene expression in human MDM

To investigate the potential role of $P2X_4$ in cytokines and chemokines expression in MDMs, an RT^2 profiler PCR array which screened for 84 different genes was performed following stimulation with 100 μM ATP in the presence or absence of 10 μM PSB-12062 for 6h. MDMs were also stimulated with100 ng/mL of LPS for 6h, as a positive control. A heat map summarizing the gene expression data for 76 different genes are illustrated in Figure 4A. Eight genes (BMP4, CXCL10, CXCL11, CXCL12, IL2, IL17A, TNFRSF11B and XCL1) were excluded from the heat map as they were found at undetectable levels in all conditions (unstimulated, 100 μM ATP and 100 ng/mL LPS). Interestingly, the majority of the genes investigated were found to be constitutively expressed in MDMs (data not shown) while stimulation of MDMs with 100 μM ATP resulted in the induction of various genes, with CXCL2, CXCL5, IL-12α, IL-12β, OSM, PPBP and TGF-β2 being positively induced (Figure 4B). As a positive control, 100 ng/mL LPS significantly upregulated the mRNA expression of no less than 35 genes as indicated in red in Figure 4A. In addition to this, the effect of 100 μM ATP stimulation was investigated at the protein level for several cytokines and chemokines, though no significance was observed (Supplementary Figure 3). Out of the proteins investigated, one chemokine (Eotaxin) and eleven cytokines (IL-13, IL-9, IL-4, IL-5, IFN-γ, IL-12p70, IL-17A, IL-33, IL-23A, IL-6 and IL-17E) were found to be below the detectable range (data not shown).

To identify potential candidates, several criteria were applied. These criteria included genes that were: 1) induced by stimulation of ATP, 2) was unaffected by pre-treatment of

antagonist (10 μM PSB-12062) alone, and 3) had their mRNA expression altered when the antagonist was present together with the agonist. Taking these criteria together allowed the identification of CXCL5 as a candidate gene for further study in the MDMs. ATP induced a time-dependent increase in mRNA expression of CXCL5 in MDM across four different time-points (6h, 9h, 18h and 24h) with expression peaking at 24h time-point (23.5 ± 5.0 fold upregulation, N=4; Figure 4C). Having identified a role for $P2X_4$ receptor in modulating CXCL5 mRNA expression, we further investigated its effects at the protein level. Similar to mRNA expression, stimulation of MDMs with ATP also caused a time-dependent increase in CXCL5 protein secretion as quantified by ELISA across four different time-points (0h, 24h, 32h and 48h) with secretion peaking at 48h time-point (686.9 ± 148.3 pg/mL, N=7, $P<0.01$; Figure 4D). The level of secreted CXCL5 protein was only detectable at higher time-points as 6h and 9h yield no significant secretion (data not shown).

ATP-induced CXCL5 mRNA expression and protein secretion is modulated by the activation of $P2X_4$

In the presence of ATP, pre-treatment of MDM with PSB-12062 caused a significant reduction in ATP-induced CXCL5 mRNA expression at lower time-points (6h = 40.4 ± 4.9% reduction, N=5, $P<0.01$ and 9h = 34.8 ± 7.2 % reduction, N=4, $P<0.05$; Figure 5A). This inhibition was found to be translated to the protein level as pre-treatment of MDM with PSB-12062 also caused a significant reduction in ATP-induced CXCL5 secretion at higher time-points (32h = 22.9 ± 8.5 % reduction, N=6, $P<0.01$ and 48h = 30.70 ± 6.29 % reduction, N=7, $P<0.001$; Figure 5B and C). To ensure the selectivity of the compound, we also investigated the effect of lower concentrations of PSB-12062 on MDM cells. PSB-12062 caused a concentration-dependent inhibition in ATP-induced CXCL5 secretion at 48h (1 μM = 12.0 ± 4.6 % inhibition, N=3, $P<0.05$, 5 μM = 26.4 ± 7.2 % inhibition, N=4, $P<0.05$; Figure 5D). Similar to the inhibitory effect observed in the presence of PSB-12062, pre-treatment of MDMs with 5 μM BX-430 caused a significant inhibition in ATP-induced CXCL5 secretion at 48h (20.07 ± 2.05 % inhibition, N=7, $P<0.01$; Figure 5E).

In addition to this, the effect of IVM was also tested on MDMs prior to stimulation with ATP. Pre-treatment of MDMs with IVM caused a significant increase in the amount of CXCL5 protein secretion at 48h time-point (26.48 ± 10.70 % potentiation, N=6, $P<0.05$; Figure 5F). In an effort to understand the mechanism by which $P2X_4$ receptor stimulates CXCL5 secretion, we performed experiments in the absence of extracellular Ca^{2+} to investigate a dependency upon Ca^{2+} influx. In these experiments, the absence of extracellular Ca^{2+} caused a significant reduction in ATP-induced CXCL5 secretion (41.80 ± 5.36 % inhibition, 48 hours; N=7, $P<0.001$; Figure 5G) versus control experiments in the presence of extracellular Ca^{2+}. Furthermore, the inhibitory action of PSB-12062 and BX430 on ATP-induced CXCL5 secretion was lost in the absence of extracellular Ca^{2+} (Figure 5H). Together, these data illustrated a role of $P2X_4$ receptor activation in the modulation of ATP-induced CXCL5 mRNA expression and secretion.

$P2X_7$, $P2Y_{11}$ and $P2Y_{13}$ receptors are not involved in the modulation of CXCL5 mRNA expression and protein secretion

To investigate the potential involvement of other P2 receptors, the effect of $P2X_7$, $P2Y_{11}$ and $P2Y_{13}$ receptor antagonists on ATP-mediated secretion of CXCL5 was studied. Pre-treatment of MDMs with A438079 (P2X7; Figure 6A), NF340 (P2Y11; Figure 6B) or MRS2211 (Figure 6C) had no significant inhibitory effect on ATP-evoked CXCL5 protein secretion. When applied together, 10 μM NF340 and 10 μM MRS2211 also had no significant effect on ATP-induced CXCL5 secretion (Figure 6D). These data illustrate that P2X7, P2Y11 and P2Y13 receptors are unlikely to play a role in modulating ATP-induced CXCL5 secretion in human MDMs.

Discussion

In the macrophage system, DAMP signals (such as ATP) work as extracellular signaling molecules that is essential for intercellular communication through activation of P2 receptors (53). Although various P2 receptors have been shown to be expressed in macrophages, it is unclear which P2 receptors are responsible for ATP-evoked $[Ca^{2+}]_i$ in human MDMs. Through qRT-PCR analysis and immunocytochemistry, the present study illustrates that human MDMs expresses four P2X receptors, $P2X_1$, $P2X_4$, $P2X_5$, and $P2X_7$, and all P2Y receptors, with the exception of $P2Y_{12}$ and $P2Y_{14}$. Our data corroborates previous finding which reported the presence of all P2 receptors except $P2Y_{12}$, $P2X_2$, $P2X_3$ and $P2X_6$ on human alveolar macrophages (54). Next, Ca^{2+} experiments were used as an indication that functional P2X and P2Y receptors were present on human MDM cells. Through intracellular Ca^{2+} measurements of Fura-2 AM loaded cells, we have showed that ATP-induced $[Ca^{2+}]_i$ response in human MDM exhibited a biphasic kinetic. The first component of the $[Ca^{2+}]_i$ response showed features of a metabotropic mechanism, lacking dependence on extracellular calcium and high sensitivity towards PLC inhibition. In addition to this, the activation of $P2Y_{11}$ and $P2Y_{13}$ receptors appeared to be essential for the amplitude of the ATP-evoked $[Ca^{2+}]_i$ response in human MDMs. Treatment of MDMs with antagonists for $P2Y_1$, $P2Y_2$ and $P2Y_6$ did not have any effect on the amplitude and decay phase of the ATP-evoked Ca^{2+} response in macrophages suggestive of their limited role. This was an interesting observation as $P2Y_2$ and $P2Y_6$ appear to have been found functional through intracellular Ca^{2+} measurements in monocytes and PBMCs (55, 56). The second delayed phase of ATP-evoked $[Ca^{2+}]_i$ response exhibited characteristics of an ionotropic response with $P2X_4$ receptor, but not $P2X_1$ or $P2X_7$ receptors, contributing to this response. Selective $P2X_4$ receptor antagonists, PSB-12062 and BX430 significantly accelerated the decay kinetics of the Ca^{2+} response, causing a consequential reduction in area under the curve and reducing the time it takes for the ATP-evoked Ca^{2+} decay response to return to the baseline. Although Norenberg et al. (2012) identified that IVM was also able to potentiate currents of human $P2X_7$ receptor in human MDM, it was clarified that the effect it has on delaying decay of currents is specific for $P2X_4$ receptor (50). In our MDM system, we were able to illustrate that IVM potentiated not only the amplitude of the $[Ca^{2+}]_i$ response but also delay of the decay kinetics. The effect of IVM in increasing the duration of $[Ca^{2+}]_i$ are therefore inconsistent with a role for $P2X_7$, furthermore 100 μM ATP is significantly below the activation

threshold for $P2X_7$ (13). The effect of IVM is consistent with positive allosteric modulation of $P2X_4$ (9, 57).

Transcriptional profiler array study identified that in human MDMs, 100 μM ATP induced the expression of various cytokine and chemokine genes that are relevant to the immune system, with CXCL5 being a major candidate that was studied further. To the best of our knowledge, there has been no reported evidence that human monocyte-derived macrophages are able to synthesize and secrete CXCL5 in response to ATP stimulation. CXCL5, a ligand of CXCR2 receptor, is typically expressed in inflammatory cells in various tissues (58). They belong to CXC family of chemoattractant molecules specialized in the modulation of neutrophil chemotaxis and chemokine scavenging (59, 60). Here, we showed that human MDMs are not only able to transcriptionally express mRNA of CXCL5 genes but also synthesize and secrete CXCL5 protein, in a time-dependent manner. This expression and secretion of CXCL5 was found to be modulated by the activation of $P2X_4$, as illustrated by the effect of IVM and PSB-12062. However, as the PSB-12062 effect was only observed at higher time points (post 32h), it is likely that rather than regulating the secretion of CXCL5, $P2X_4$ activation modulates the synthesis of ATP-induced CXCL5. In addition to this, we also tested the possible involvement of other purinergic receptors on ATP-induced CXCL5 secretion. The lack of effect of selective antagonists for $P2X_7$, $P2Y_{11}$ and $P2Y_{13}$ receptors indicate that these receptors are not involved in modulating the secretion of CXCL5 in human MDMs, despite their potential involvement in ATP-evoked $[Ca^{2+}]_i$ response. Earlier studies by a group found that elevation in $[Ca^{2+}]_i$ is required, but not necessarily sufficient for the release of certain cytokines and chemokines in brain macrophages (microglia) (61). The lack of involvement of $P2Y_{11}$ and $P2Y_{13}$ receptor in mediating ATP-driven CXCL5 secretion led to the hypothesis that it may involve a process independent of calcium level. However, when the level of ATP-induced CXCL5 secretion was investigated in conditions where extracellular Ca^{2+} was removed, we found that there was a significant inhibition in secreted CXCL5 level and to our surprise, to a similar level obtained when $P2X_4$ receptor was blocked with either PSB-12062 or BX-430. More interestingly, in the absence of extracellular Ca^{2+}, the inhibitory action of $P2X_4$ antagonists was lost. Altogether, these observations demonstrate that ATP-induced CXCL5 secretion in human MDMs is dependent on Ca^{2+} influx via the $P2X_4$ receptor.

It was not until very recently that the mechanism involved downstream of CXCL5 was revealed in greater detail. CXCL5 has been shown to activate ERK, JNK, p38 MAPK signaling pathways, all of which are key players in tumour growth and metastasis (62). In the context of inflammatory diseases, CXCL5 have been shown to offer an atheroprotective role by enhancing cholesterol efflux capacity of macrophages and regulating foam cell formation (63). More recent studies revealed that tissue-resident $CCR2^+$ MDMs are essential mediators of neutrophil recruitment into ischemic myocardia tissue. This process is mediated by a TLR9/MyD88/CXCL5 pathway with CXCL5 playing a critical role in guiding neutrophil crawling, as shown through photon imaging system (64). In this present study, we are able to consider that upon stimulation with DAMP signal, human MDMs synthesize and secrete CXCL5, which can then in turn activate neutrophils and recruit them to sites of injury. Although the mechanism by which $P2X_4$ receptor activation modulates expression and secretion of CXCL5 in human MDM has not been investigated here, several

speculations can be made. Studies by Song et al. (2012) illustrated that pro-inflammatory chemokine CXCL5 was found to be rapidly upregulated by local presence of IL-1β and that its action was potentiated by MMP-2 and MMP-9, working synergistically to initiate neutrophil recruitment (65). It is possible that $P2X_4$ receptor activation modulates ATP-induced CXCL5 secretion by regulating IL-1β levels. Recent structural and functional studies provided evidences of possible interactions of $P2X_4$ receptor with $P2X_7$ receptor in macrophages which was followed by a study illustrating that the expression of $P2X_4$ receptor is required for $P2X_7$ receptor-dependent IL-1β release in mouse bone marrow-derived dendritic cells (66, 67). In addition to this, a study by Zineh, et al. (68) illustrated that treatment of HUVECs with atorvastatin reduced IL-1β-induced CXCL5 levels in a concentration-dependent manner. Whether this effect involve $P2X_4$ activity is unclear, however, treatment of human monocytes with fluvastatin have resulted in suppression of $P2X_4$ activity through depletion of cholesterol levels (69). Further studies will undoubtedly be required to unravel the mechanism by which $P2X_4$ regulates CXCL5 synthesis and secretion in human macrophages. Of further interest is the recent identification of CXCL5 as mediator in inflammatory pain arising from UVB irradiation of skin (sun burn) (70).

In conclusion, our data show that both P2X and P2Y receptors are responsible for ATP-evoked $[Ca^{2+}]_i$ response in human MDMs. $P2Y_{11}$ and $P2Y_{13}$ receptor activation underlies the amplitude of ATP-evoked $[Ca^{2+}]_i$ response, whereas $P2X_4$ receptor activity is responsible for the duration of Ca^{2+} response. Additionally, we have elucidated a potential role for $P2X_4$ receptor as a modulator of ATP-induced CXCL5 expression and secretion in human MDMs which may be important in the recruitment of neutrophils. Although additional work will be required to uncover the mechanism of $P2X_4$-CXCL5 interaction in human macrophages, the current study exposed a novel role of $P2X_4$ in human macrophages and its contribution towards the innate immune system.

Supplementary Material

Refer to Web version on PubMed Central for supplementary material.

Acknowledgements

This manuscript is funded by the Biotechnology and Biological Sciences Research Council (BBSRC).

Abbreviations

MDM	Monocyte-derived macrophages
IVM	Ivermectin
AUC	Area under the curve
DAMP	Danger-Associated Molecular Pattern

References

1. Rubartelli A, Lotze MT. Inside, outside, upside down: damage-associated molecular-pattern molecules (DAMPs) and redox. Trends Immunol. 2007; 28:429–436. [PubMed: 17845865]

2. Shi Y, Evans JE, Rock KL. Molecular identification of a danger signal that alerts the immune system to dying cells. Nature. 2003; 425:516–521. [PubMed: 14520412]
3. Cekic C, Linden J. Purinergic regulation of the immune system. Nature reviews Immunology. 2016; 16:177–192.
4. Burnstock G, Williams M. P2 purinergic receptors: modulation of cell function and therapeutic potential. The Journal of pharmacology and experimental therapeutics. 2000; 295:862–869. [PubMed: 11082418]
5. Jacobson KA, Ivanov AA, de Castro S, Harden TK, Ko H. Development of selective agonists and antagonists of P2Y receptors. Purinergic signalling. 2009; 5:75–89. [PubMed: 18600475]
6. Bhatt DL, Topol EJ. Scientific and therapeutic advances in antiplatelet therapy. Nat Rev Drug Discov. 2003; 2:15–28. [PubMed: 12509756]
7. Burnstock G, Boeynaems JM. Purinergic signalling and immune cells. Purinergic signalling. 2014; 10:529–564. [PubMed: 25352330]
8. Jacob F, Perez Novo C, Bachert C, Van Crombruggen K. Purinergic signaling in inflammatory cells: P2 receptor expression, functional effects, and modulation of inflammatory responses. Purinergic signalling. 2013; 9:285–306. [PubMed: 23404828]
9. Fountain SJ, North RA. A C-terminal lysine that controls human P2X4 receptor desensitization. The Journal of biological chemistry. 2006; 281:15044–15049. [PubMed: 16533808]
10. Dubyak GR. Go it alone no more--P2X7 joins the society of heteromeric ATP-gated receptor channels. Molecular pharmacology. 2007; 72:1402–1405. [PubMed: 17895406]
11. Hong S, Schwarz N, Brass A, Seman M, Haag F, Koch-Nolte F, Schilling WP, Dubyak GR. Differential regulation of P2X7 receptor activation by extracellular nicotinamide adenine dinucleotide and ecto-ADP-ribosyltransferases in murine macrophages and T cells. Journal of immunology. 2009; 183:578–592.
12. Khakh BS, North RA. P2X receptors as cell-surface ATP sensors in health and disease. Nature. 2006; 442:527–532. [PubMed: 16885977]
13. North RA. Molecular physiology of P2X receptors. Physiological reviews. 2002; 82:1013–1067. [PubMed: 12270951]
14. Kawano A, Tsukimoto M, Mori D, Noguchi T, Harada H, Takenouchi T, Kitani H, Kojima S. Regulation of P2X7-dependent inflammatory functions by P2X4 receptor in mouse macrophages. Biochemical and biophysical research communications. 2012; 420:102–107. [PubMed: 22405772]
15. Kawano A, Tsukimoto M, Noguchi T, Hotta N, Harada H, Takenouchi T, Kitani H, Kojima S. Involvement of P2X4 receptor in P2X7 receptor-dependent cell death of mouse macrophages. Biochemical and biophysical research communications. 2012; 419:374–380. [PubMed: 22349510]
16. McGaraughty S, Chu KL, Namovic MT, Donnelly-Roberts DL, Harris RR, Zhang XF, Shieh CC, Wismer CT, Zhu CZ, Gauvin DM, Fabiyi AC, et al. P2X7-related modulation of pathological nociception in rats. Neuroscience. 2007; 146:1817–1828. [PubMed: 17478048]
17. Pelegrin P, Barroso-Gutierrez C, Surprenant A. P2X7 receptor differentially couples to distinct release pathways for IL-1beta in mouse macrophage. Journal of immunology. 2008; 180:7147–7157.
18. Qu Y, Franchi L, Nunez G, Dubyak GR. Nonclassical IL-1 beta secretion stimulated by P2X7 receptors is dependent on inflammasome activation and correlated with exosome release in murine macrophages. Journal of immunology. 2007; 179:1913–1925.
19. Raouf R, Chabot-Dore AJ, Ase AR, Blais D, Seguela P. Differential regulation of microglial P2X4 and P2X7 ATP receptors following LPS-induced activation. Neuropharmacology. 2007; 53:496–504. [PubMed: 17675190]
20. Ulmann L, Hirbec H, Rassendren F. P2X4 receptors mediate PGE2 release by tissue-resident macrophages and initiate inflammatory pain. The EMBO journal. 2010; 29:2290–2300. [PubMed: 20562826]
21. Gu BJ, Baird PN, Vessey KA, Skarratt KK, Fletcher EL, Fuller SJ, Richardson AJ, Guymer RH, Wiley JS. A rare functional haplotype of the P2RX4 and P2RX7 genes leads to loss of innate phagocytosis and confers increased risk of age-related macular degeneration. FASEB journal : official publication of the Federation of American Societies for Experimental Biology. 2013; 27:1479–1487. [PubMed: 23303206]

22. Fujiwara N, Kobayashi K. Macrophages in inflammation. Curr Drug Targets Inflamm Allergy. 2005; 4:281–286. [PubMed: 16101534]
23. Arango Duque G, Descoteaux A. Macrophage cytokines: involvement in immunity and infectious diseases. Front Immunol. 2014; 5:491. [PubMed: 25339958]
24. Jeyaseelan S, Manzer R, Young SK, Yamamoto M, Akira S, Mason RJ, Worthen GS. Induction of CXCL5 during inflammation in the rodent lung involves activation of alveolar epithelium. Am J Respir Cell Mol Biol. 2005; 32:531–539. [PubMed: 15778492]
25. Koltsova EK, Ley K. The mysterious ways of the chemokine CXCL5. Immunity. 2010; 33:7–9. [PubMed: 20643334]
26. Chavey C, Fajas L. CXCL5 drives obesity to diabetes, and further. Aging (Albany NY). 2009; 1:674–677. [PubMed: 20157549]
27. Groot-Kormelink PJ, Fawcett L, Wright PD, Gosling M, Kent TC. Quantitative GPCR and ion channel transcriptomics in primary alveolar macrophages and macrophage surrogates. BMC immunology. 2012; 13:57. [PubMed: 23102269]
28. Li J, Pritchard DK, Wang X, Park DR, Bumgarner RE, Schwartz SM, Liles WC. cDNA microarray analysis reveals fundamental differences in the expression profiles of primary human monocytes, monocyte-derived macrophages, and alveolar macrophages. Journal of leukocyte biology. 2007; 81:328–335. [PubMed: 17046970]
29. Jin M, Opalek JM, Marsh CB, Wu HM. Proteome comparison of alveolar macrophages with monocytes reveals distinct protein characteristics. Am J Respir Cell Mol Biol. 2004; 31:322–329. [PubMed: 15130903]
30. Tomechko SE, Lundberg KC, Jarvela J, Bebek G, Chesnokov NG, Schlatzer D, Ewing RM, Boom WH, Chance MR, Silver RF. Proteomic and bioinformatics profile of paired human alveolar macrophages and peripheral blood monocytes. Proteomics. 2015; 15:3797–3805. [PubMed: 26389541]
31. Donnelly LE, Tudhope SJ, Fenwick PS, Barnes PJ. Effects of formoterol and salmeterol on cytokine release from monocyte-derived macrophages. The European respiratory journal. 2010; 36:178–186. [PubMed: 19926732]
32. Sarir H, Mortaz E, Karimi K, Johnson M, Nijkamp FP, Folkerts G. Combination of fluticasone propionate and salmeterol potentiates the suppression of cigarette smoke-induced IL-8 production by macrophages. European journal of pharmacology. 2007; 571:55–61. [PubMed: 17631879]
33. Komuro I, Keicho N, Iwamoto A, Akagawa KS. Human alveolar macrophages and granulocyte-macrophage colony-stimulating factor-induced monocyte-derived macrophages are resistant to H2O2 via their high basal and inducible levels of catalase activity. The Journal of biological chemistry. 2001; 276:24360–24364. [PubMed: 11313354]
34. Ginhoux F, Jung S. Monocytes and macrophages: developmental pathways and tissue homeostasis. Nature reviews Immunology. 2014; 14:392–404.
35. Wynn TA. Integrating mechanisms of pulmonary fibrosis. The Journal of experimental medicine. 2011; 208:1339–1350. [PubMed: 21727191]
36. Wynn TA, Barron L. Macrophages: master regulators of inflammation and fibrosis. Semin Liver Dis. 2010; 30:245–257. [PubMed: 20665377]
37. Murray PJ, Wynn TA. Protective and pathogenic functions of macrophage subsets. Nature reviews Immunology. 2011; 11:723–737.
38. Liang J, Jung Y, Tighe RM, Xie T, Liu N, Leonard M, Gunn MD, Jiang D, Noble PW. A macrophage subpopulation recruited by CC chemokine ligand-2 clears apoptotic cells in noninfectious lung injury. Am J Physiol Lung Cell Mol Physiol. 2012; 302:L933–940. [PubMed: 22287613]
39. Moore BB, Paine R 3rd, Christensen PJ, Moore TA, Sitterding S, Ngan R, Wilke CA, Kuziel WA, Toews GB. Protection from pulmonary fibrosis in the absence of CCR2 signaling. Journal of immunology. 2001; 167:4368–4377.
40. Gharaee-Kermani M, McCullumsmith RE, Charo IF, Kunkel SL, Phan SH. CC-chemokine receptor 2 required for bleomycin-induced pulmonary fibrosis. Cytokine. 2003; 24:266–276. [PubMed: 14609568]

41. Shichino S, Abe J, Ueha S, Otsuji M, Tsukui T, Kosugi-Kanaya M, Shand FH, Hashimoto S, Suzuki HI, Morikawa T, Inagaki Y, et al. Reduced supply of monocyte-derived macrophages leads to a transition from nodular to diffuse lesions and tissue cell activation in silica-induced pulmonary fibrosis in mice. The American journal of pathology. 2015; 185:2923–2938. [PubMed: 26456580]
42. Agostini C, Gurrieri C. Chemokine/cytokine cocktail in idiopathic pulmonary fibrosis. Proc Am Thorac Soc. 2006; 3:357–363. [PubMed: 16738201]
43. Tasaka S, Mizoguchi K, Funatsu Y, Namkoong H, Yamasawa W, Ishii M, Hasegawa N, Betsuyaku T. Cytokine profile of bronchoalveolar lavage fluid in patients with combined pulmonary fibrosis and emphysema. Respirology. 2012; 17:814–820. [PubMed: 22515655]
44. Baj-Krzyworzeka M, Mytar B, Szatanek R, Surmiak M, Weglarczyk K, Baran J, Siedlar M. Colorectal cancer-derived microvesicles modulate differentiation of human monocytes to macrophages. J Transl Med. 2016; 14:36. [PubMed: 26838097]
45. Babu R, Brown A. A consensus surface activation marker signature is partially dependent on human immunodeficiency virus type 1 Nef expression within productively infected macrophages. Retrovirology. 2013; 10:155. [PubMed: 24341794]
46. Waldo SW, Li Y, Buono C, Zhao B, Billings EM, Chang J, Kruth HS. Heterogeneity of human macrophages in culture and in atherosclerotic plaques. The American journal of pathology. 2008; 172:1112–1126. [PubMed: 18321997]
47. Eligini S, Crisci M, Bono E, Songia P, Tremoli E, Colombo GI, Colli S. Human monocyte-derived macrophages spontaneously differentiated in vitro show distinct phenotypes. Journal of cellular physiology. 2013; 228:1464–1472. [PubMed: 23255209]
48. Kruger M, Van de Winkel JG, De Wit TP, Coorevits L, Ceuppens JL. Granulocyte-macrophage colony-stimulating factor down-regulates CD14 expression on monocytes. Immunology. 1996; 89:89–95. [PubMed: 8911145]
49. Sadeghi K, Wisgrill L, Wessely I, Diesner SC, Schuller S, Durr C, Heinle A, Sachet M, Pollak A, Forster-Waldl E, Spittler A. GM-CSF Down-Regulates TLR Expression via the Transcription Factor PU.1 in Human Monocytes. PloS one. 2016; 11 e0162667.
50. Norenberg W, Sobottka H, Hempel C, Plotz T, Fischer W, Schmalzing G, Schaefer M. Positive allosteric modulation by ivermectin of human but not murine P2X7 receptors. British journal of pharmacology. 2012; 167:48–66. [PubMed: 22506590]
51. Hernandez-Olmos V, Abdelrahman A, El-Tayeb A, Freudendahl D, Weinhausen S, Muller CE. N-substituted phenoxazine and acridone derivatives: structure-activity relationships of potent P2X4 receptor antagonists. Journal of medicinal chemistry. 2012; 55:9576–9588. [PubMed: 23075067]
52. Ase AR, Honson NS, Zaghdane H, Pfeifer TA, Seguela P. Identification and characterization of a selective allosteric antagonist of human P2X4 receptor channels. Molecular pharmacology. 2015; 87:606–616. [PubMed: 25597706]
53. Zhang X, Mosser DM. Macrophage activation by endogenous danger signals. The Journal of pathology. 2008; 214:161–178. [PubMed: 18161744]
54. Myrtek D, Muller T, Geyer V, Derr N, Ferrari D, Zissel G, Durk T, Sorichter S, Luttmann W, Kuepper M, Norgauer J, et al. Activation of human alveolar macrophages via P2 receptors: coupling to intracellular Ca2+ increases and cytokine secretion. Journal of immunology. 2008; 181:2181–2188.
55. Campwala H, Sexton DW, Crossman DC, Fountain SJ. P2Y(6) receptor inhibition perturbs CCL2-evoked signalling in human monocytic and peripheral blood mononuclear cells. Journal of cell science. 2014; 127:4964–4973. [PubMed: 25271060]
56. Bowler JW, Bailey RJ, North RA, Surprenant A. P2X4, P2Y1 and P2Y2 receptors on rat alveolar macrophages. British journal of pharmacology. 2003; 140:567–575. [PubMed: 12970084]
57. Priel A, Silberberg SD. Mechanism of ivermectin facilitation of human P2X4 receptor channels. The Journal of general physiology. 2004; 123:281–293. [PubMed: 14769846]
58. Wu X, Mimms R, Lima R, Peters-Hall J, Rose MC, Pena MT. Localization of inflammatory mediators in pediatric sinus mucosa. Archives of otolaryngology--head & neck surgery. 2012; 138:389–397. [PubMed: 22508623]

59. Keates S, Keates AC, Mizoguchi E, Bhan A, Kelly CP. Enterocytes are the primary source of the chemokine ENA-78 in normal colon and ulcerative colitis. The American journal of physiology. 1997; 273:G75–82. [PubMed: 9252512]
60. Mei J, Liu Y, Dai N, Favara M, Greene T, Jeyaseelan S, Poncz M, Lee JS, Worthen GS. CXCL5 regulates chemokine scavenging and pulmonary host defense to bacterial infection. Immunity. 2010; 33:106–117. [PubMed: 20643340]
61. Hoffmann A, Kann O, Ohlemeyer C, Hanisch UK, Kettenmann H. Elevation of basal intracellular calcium as a central element in the activation of brain macrophages (microglia): suppression of receptor-evoked calcium signaling and control of release function. The Journal of neuroscience : the official journal of the Society for Neuroscience. 2003; 23:4410–4419. [PubMed: 12805281]
62. Dai Z, Wu J, Chen F, Cheng Q, Zhang M, Wang Y, Guo Y, Song T. CXCL5 promotes the proliferation and migration of glioma cells in autocrine- and paracrine-dependent manners. Oncol Rep. 2016
63. Rousselle A, Qadri F, Leukel L, Yilmaz R, Fontaine JF, Sihn G, Bader M, Ahluwalia A, Duchene J. CXCL5 limits macrophage foam cell formation in atherosclerosis. The Journal of clinical investigation. 2013; 123:1343–1347. [PubMed: 23376791]
64. Li W, Hsiao HM, Higashikubo R, Saunders BT, Bharat A, Goldstein DR, Krupnick AS, Gelman AE, Lavine KJ, Kreisel D. Heart-resident CCR2+ macrophages promote neutrophil extravasation through TLR9/MyD88/CXCL5 signaling. JCI Insight. 2016; 1
65. Song J, Wu C, Zhang X, Sorokin LM. In vivo processing of CXCL5 (LIX) by matrix metalloproteinase (MMP)-2 and MMP-9 promotes early neutrophil recruitment in IL-1beta-induced peritonitis. Journal of immunology. 2013; 190:401–410.
66. Perez-Flores G, Levesque SA, Pacheco J, Vaca L, Lacroix S, Perez-Cornejo P, Arreola J. The P2X7/P2X4 interaction shapes the purinergic response in murine macrophages. Biochemical and biophysical research communications. 2015; 467:484–490. [PubMed: 26456657]
67. Sakaki H, Fujiwaki T, Tsukimoto M, Kawano A, Harada H, Kojima S. P2X4 receptor regulates P2X7 receptor-dependent IL-1beta and IL-18 release in mouse bone marrow-derived dendritic cells. Biochemical and biophysical research communications. 2013; 432:406–411. [PubMed: 23428419]
68. Zineh I, Beitelshees AL, Welder GJ, Hou W, Chegini N, Wu J, Cresci S, Province MA, Spertus JA. Epithelial neutrophil-activating peptide (ENA-78), acute coronary syndrome prognosis, and modulatory effect of statins. PloS one. 2008; 3 e3117.
69. Li J, Fountain SJ. Fluvastatin suppresses native and recombinant human P2X4 receptor function. Purinergic signalling. 2012; 8:311–316. [PubMed: 22222818]
70. Dawes JM, Calvo M, Perkins JR, Paterson KJ, Kiesewetter H, Hobbs C, Kaan TK, Orengo C, Bennett DL, McMahon SB. CXCL5 mediates UVB irradiation-induced pain. Science translational medicine. 2011; 3:90ra60.

Europe PMC Funders Author Manuscripts

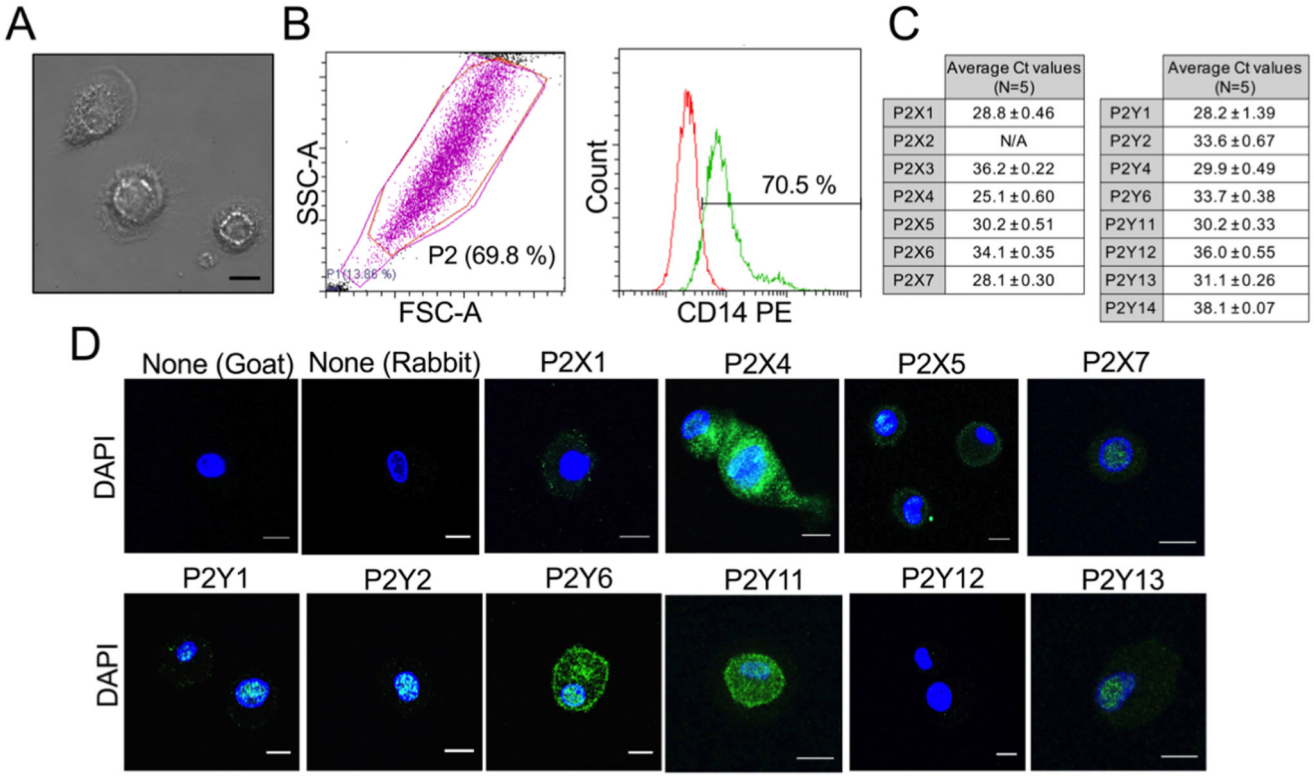

	Average Ct values (N=5)
P2X1	28.8 ± 0.46
P2X2	N/A
P2X3	36.2 ± 0.22
P2X4	25.1 ± 0.60
P2X5	30.2 ± 0.51
P2X6	34.1 ± 0.35
P2X7	28.1 ± 0.30

	Average Ct values (N=5)
P2Y1	28.2 ± 1.39
P2Y2	33.6 ± 0.67
P2Y4	29.9 ± 0.49
P2Y6	33.7 ± 0.38
P2Y11	30.2 ± 0.33
P2Y12	36.0 ± 0.55
P2Y13	31.1 ± 0.26
P2Y14	38.1 ± 0.07

Figure 1. Characterizing GM-MDM cells and purinergic signaling in GM-MDM cells.

A) Bright field image to study morphology of GM-MDM cells resembling classical 'fried-egg' characteristics. Scale bar represents 10 μm. B) Flow cytometer analysis: FSC vs. SSC plot with P2 population indicating MDM population (left panel) and histogram to quantify $CD14^{+}$ GM-MDM cells (Red: IgG Isotype control, Green: CD14-PE; right panel). C) Level of mRNA expression of P2X and P2Y receptor genes as quantified by qRT-PCR (N=5 donors). mRNA transcript found above Ct 35 is considered absent. D) Distribution and expression of intracellular P2X and P2Y receptor proteins in GM-MDM cells as visualized under confocal microscopy. Secondary only control with either goat AF488 or Rabbit AF488 are included on the left. Scale bar represents 10 μm. Images shown in A, B and D are representative of 3 donors.

Europe PMC Funders Author Manuscripts

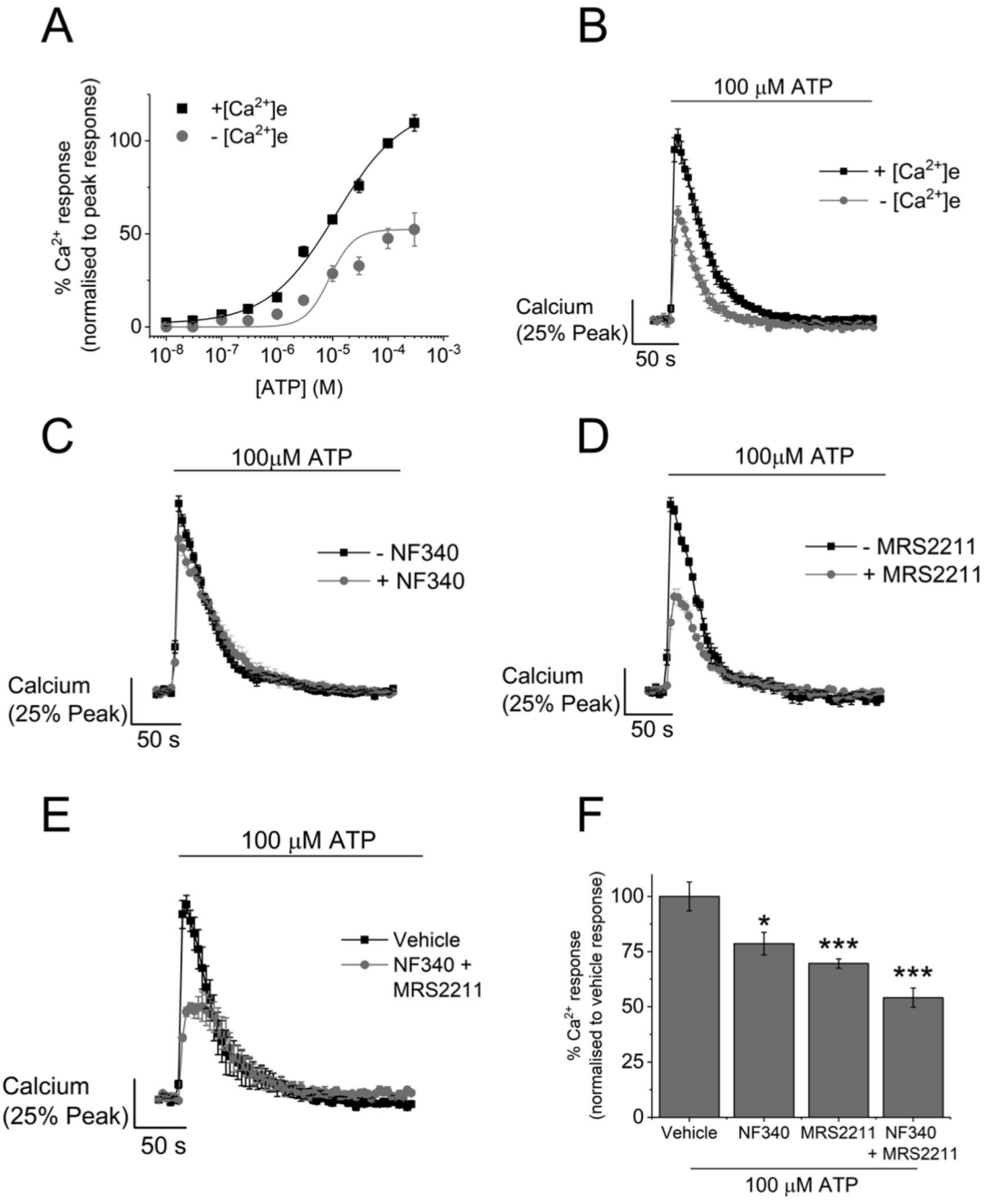

Figure 2. Activation of P2YR ($P2Y_{11}$ and $P2Y_{13}$) is responsible for the amplitude of ATP-evoked Ca^{2+} response in GM-MDM cells.

A) ATP concentration response (0.01 μM – 300 μM) in presence and absence of extracellular Ca^{2+} in GM-MDM cells (N=3 donors). B) Representative time response traces of Ca^{2+} response in response to 100 μM ATP in the presence and absence of extracellular Ca^{2+} (N=3 donors). Effect of P2Y receptor selective antagonists on ATP-evoked Ca^{2+} response: C) $P2Y_{11}$ (10 μM NF340; N=3 donors) and D) $P2Y_{13}$ (10 μM MRS2211; N=3 donors), E and F) Effect of $P2Y_{11}$ and $P2Y_{13}$ selective antagonists on ATP-evoked Ca^{2+} response (N=3 donors). Statistical significance is represented as * $p<0.05$, *** $p<0.001$

Europe PMC Funders Author Manuscripts

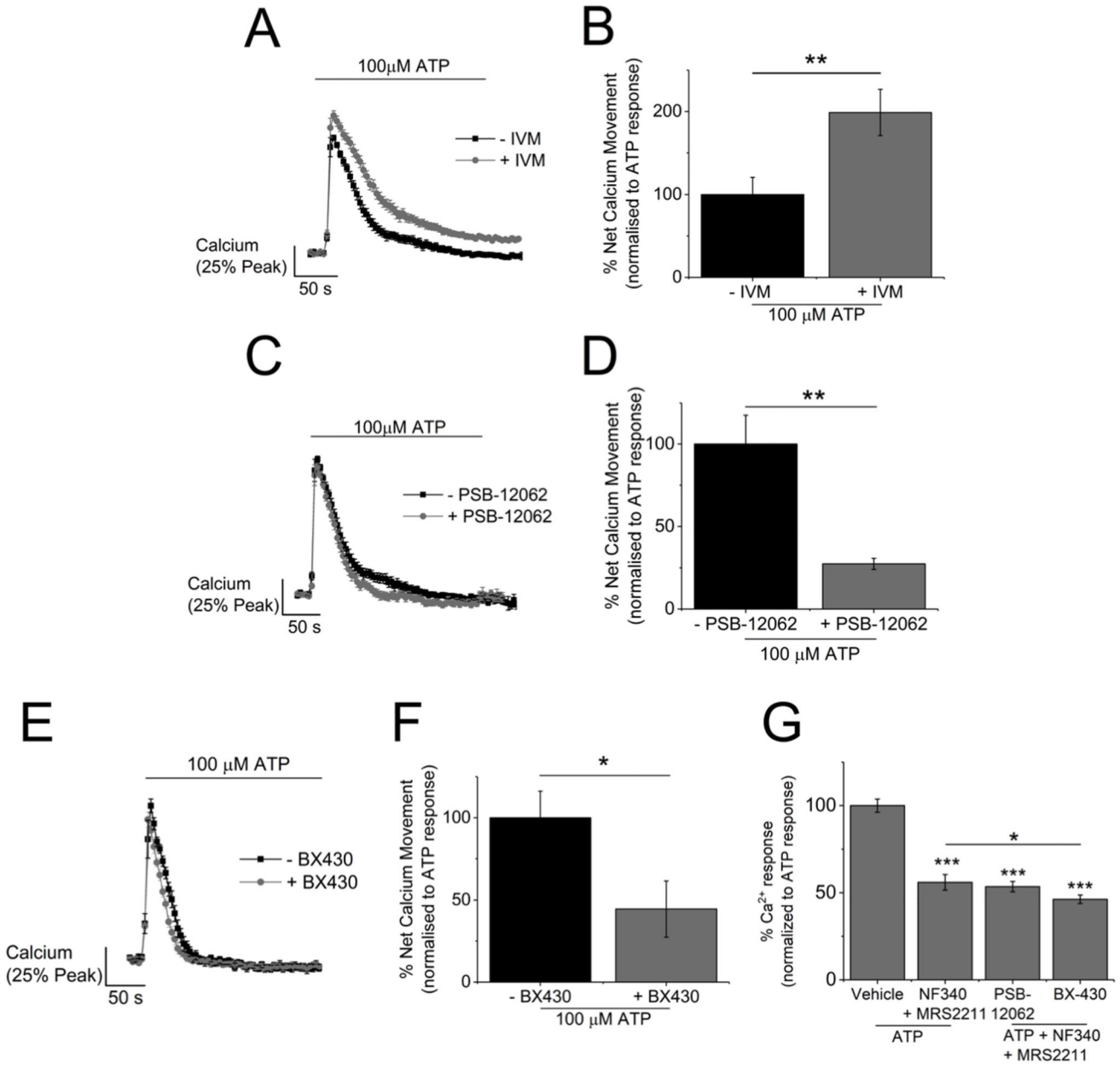

Figure 3. Activation of $P2X_4$ contribute to the sustained phase of the ATP-evoked Ca^{2+} response.

A and B) Effect of $P2X_4$ selective allosteric modulator (3 μM IVM; N=12 donors) represented as time response curves and area under the curve of Ca^{2+} response, respectively. C to F) Effect of $P2X_4$ selective antagonist, 10 μM PSB-12062 (C and D; N=12 donors) and 5 μM BX430 (E and F; N=5 donors) represented as time response curves and area under the curve of Ca^{2+} response. G) Effect of co-application of selective $P2X_4$ receptor antagonist and P2Y receptor antagonists ($P2Y_{11}$ – NF340 and $P2Y_{13}$ – MRS2211) on peak magnitude of Ca^{2+} response (N=4 donors). Statistical significance is represented as ** $p<0.01$.

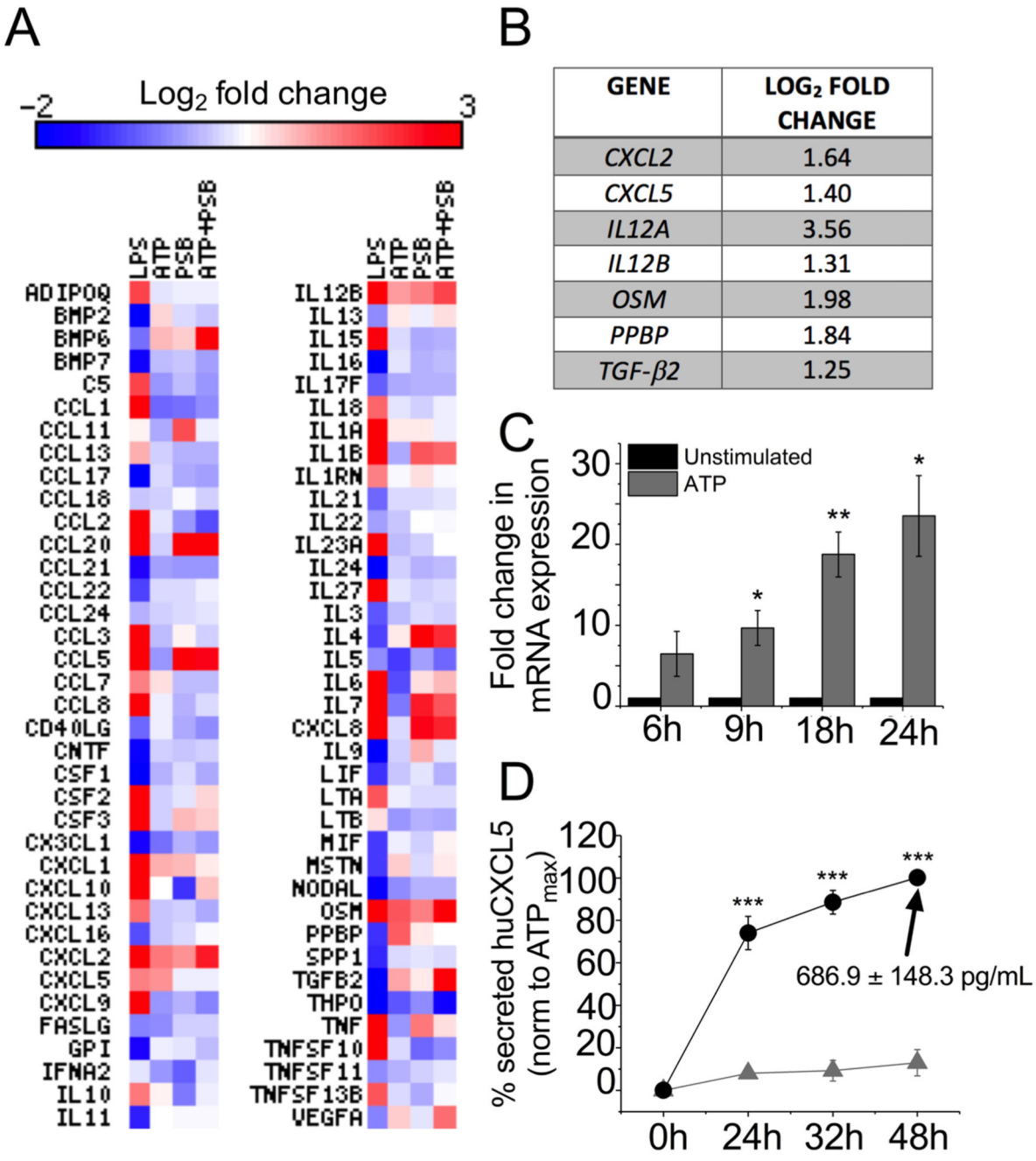

GENE	LOG$_2$ FOLD CHANGE
CXCL2	1.64
CXCL5	1.40
IL12A	3.56
IL12B	1.31
OSM	1.98
PPBP	1.84
TGF-β2	1.25

Figure 4. ATP induced the expression of various genes in human monocyte-derived macrophages.

A) Heat map summarizing expression data for 76 genes exhibiting differential expression across various stimulation (LPS, ATP, PSB-12062 and ATP + PSB-12062) at 6h. Expression of genes are presented by intensity of color as $\log_2$ fold change and averaged over 3 independent donors for all conditions, except LPS treatment consisting of 1 donor. B) ATP positively induced the expression of 7 genes. Fold change represented as Log_2 values (N=3 donors). C) qRT-PCR analysis of effect of blocking $P2X_4$ (10 μM PSB-12062) over different time points (6h, 9h, 18h and 24h) (N=6 donors). D) Time-dependent effect of ATP on

CXCL5 protein secretion as quantified using ELISA (N=7-9 donors). The absolute amount of CXCL5 secreted by maximal ATP (ATP_{max}) at 48h is indicated in black arrow. Statistical significance is represented as * $p<0.05$ and ** $p<0.01$.

Europe PMC Funders Author Manuscripts

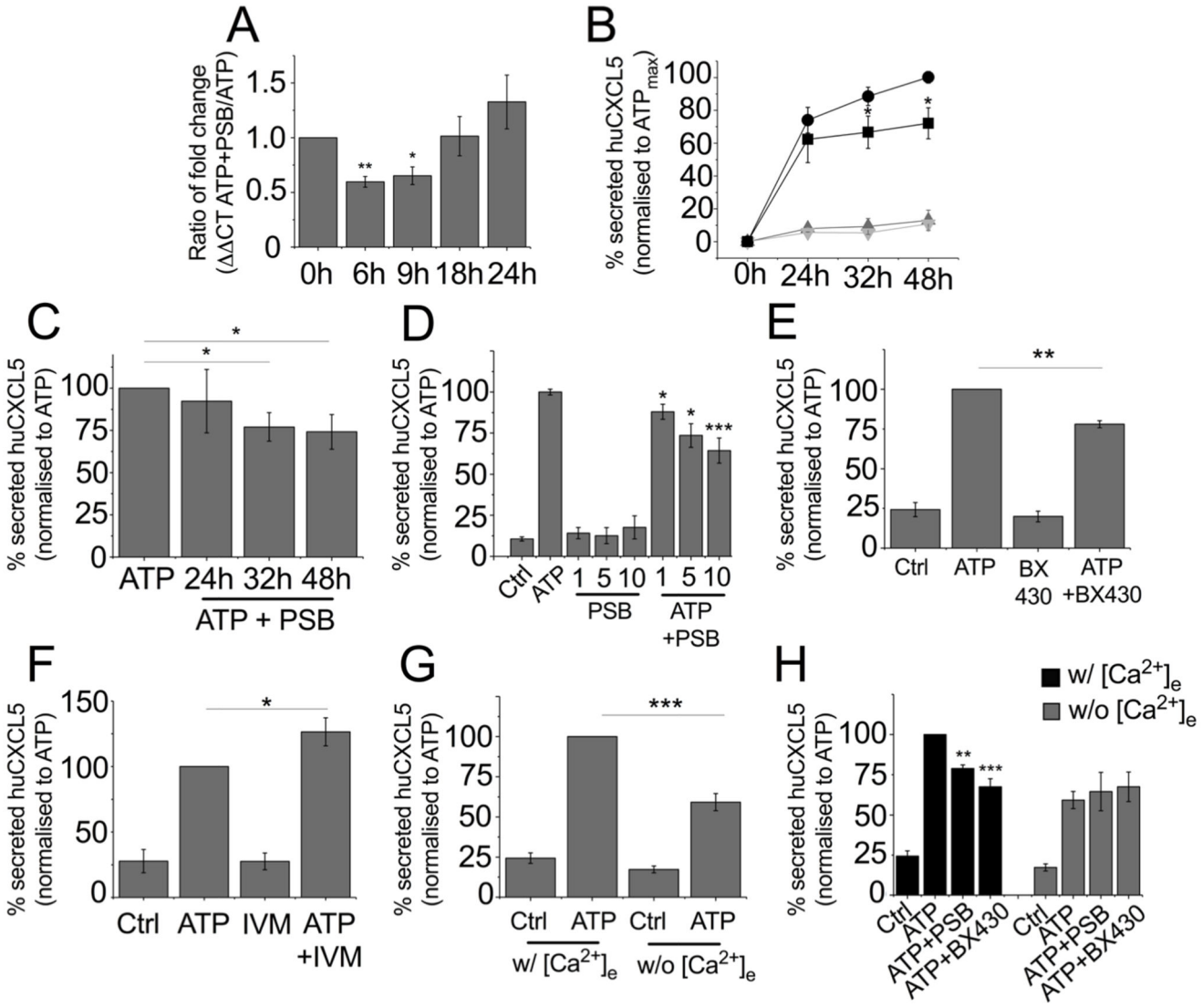

Figure 5. P2X$_4$ receptor modulates ATP-induced mRNA expression and protein secretion of CXCL5 in human MDM.

A) qRT-PCR analysis of effect of blocking P2X$_4$ (10 μM PSB-12062; N=6 donors) over different time points (6h, 9h, 18h and 24h). B & C) Effect of PSB-12062 on ATP-induced CXCL5 protein secretion at 24h (N=6 donors), 32h (N=6 donors) and 48h (N=7 donors), as quantified by ELISA. Black line: ATP control, red line: ATP + 10 μM PSB-12062, dark grey line: 10 μM PSB-12062 control, light grey line: vehicle control. D) Effect of concentration-response of PSB-12062 on ATP-induced CXCL5 protein secretion at 48h (N=4 donors). E) Effect of 5 μM BX430 on ATP-induced CXCL5 secretion at 48h (N=7 donors). F) Effect of 3 μM IVM on ATP-induced CXCL5 protein secretion at 48h (N=6 donors). G) Effect of extracellular Ca^{2+} depletion (2 mM EGTA) on constitutive and ATP-induced CXCL5 secretion (N=7 donors). H) Effect of P2X$_4$ receptor antagonists (10 μM PSB-12062 and 5 μM BX430) on ATP-induced CXCL5 secretion in the presence (N=7 donors) or absence of

extracellular Ca^{2+} (N=4 donors). Statistical significance is represented as * $p<0.05$, ** $p<0.01$ and *** $p<0.001$.

Europe PMC Funders Author Manuscripts

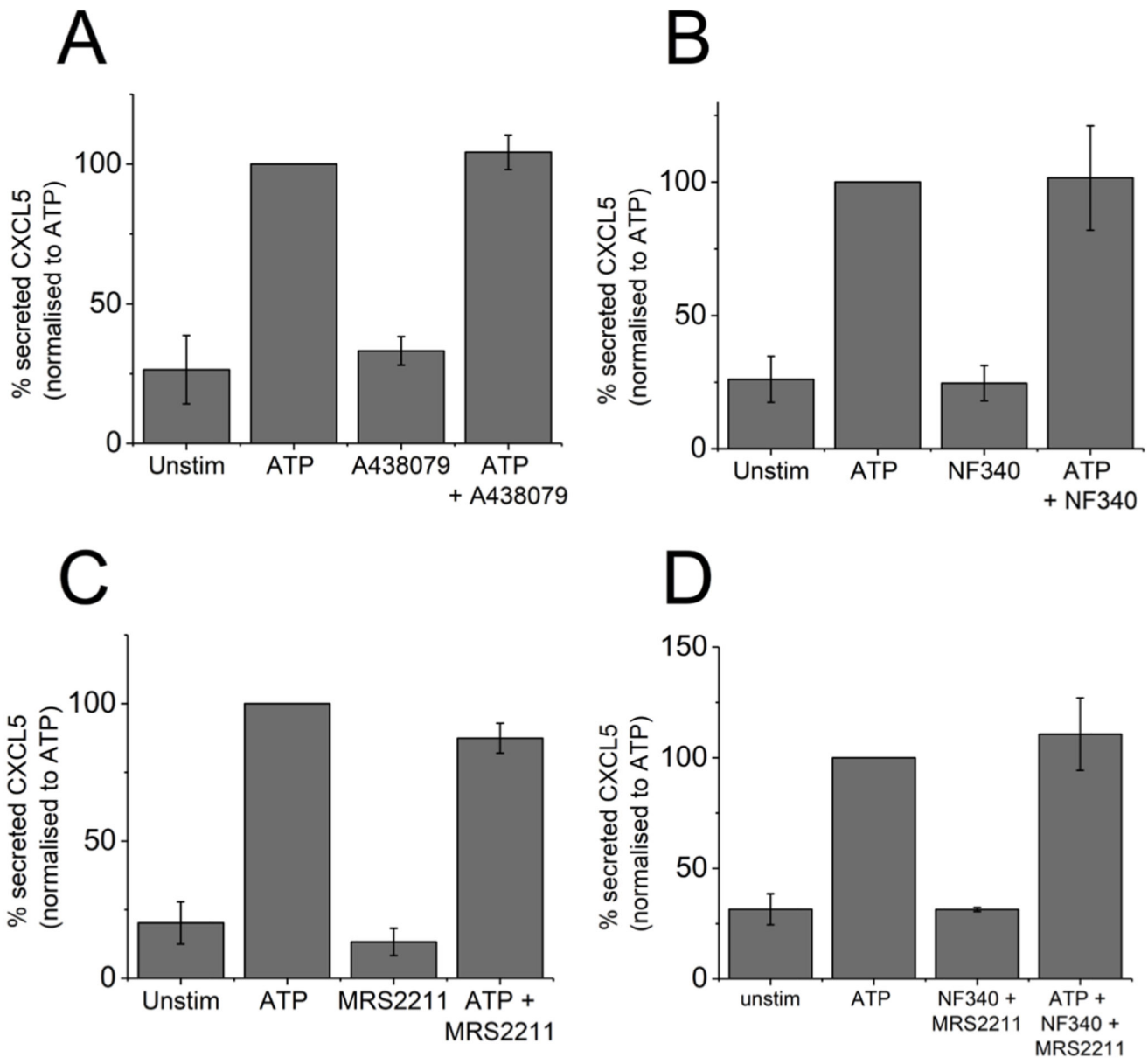

Figure 6. $P2X_7$, $P2Y_{11}$ and $P2Y_{13}$ receptor do not regulate ATP-induced protein secretion of CXCL5 at 48h in human MDM.

Effect of: A) selective $P2X_7$ receptor antagonist (5 μM A438079; N=3 donors), B) selective $P2Y_{11}$ receptor antagonist (10 μM NF340; N=4 donors), and C) selective $P2Y_{13}$ receptor antagonist (10 μM MRS2211; N=6 donors) on ATP-induced CXCL5 secretion. D) Effect of co-application of both $P2Y_{11}$ (NF340) and $P2Y_{13}$ (MRS2211) antagonists on ATP-induced CXCL5 secretion (N=3 donors).